Supporting Information

A Facile Approach to Prepare Porphyrinic Porous Aromatic Frameworks for Small Hydrocarbons Separation

*Shuang Meng, Heping Ma, Lingchang Jiang, Hao Ren, and Guangshan Zhu**

Table S1. Raw material input of PAFs

Materials	Monomer	Catalyst	Reaction Conditions	Yield (%)
PAF-40	5,10,15,20-Tetraphenylporphyrin (385mg, 0.62mmol)	$AlCl_3$ (1.6g, 4.5mmol)	$CHCl_3$, 40mL 60°C, 42h	82%
PAF-40-Fe	5,10,15,20-Tetraphenylporphyrin-Fe (400mg, 0.6mmol)			78%
PAF-40-Mn	5,10,15,20-Tetraphenylporphyrin-Mn (440mg,066mmol)			80%

5,10,15,20-Tetraphenylporphyrin (385mg, 0.62 mmol) and $AlCl_3$ (1.600 g, 4.5 mmol) was put into a 100 mL 2-neck dried flask .Then a condenser and a magnetic stirring bar was added into the flask. After degassing by Ar gas, dried $CHCl_3$ (40 mL) was added to the flask and the mixture was heated to 60 °C for 42 h under an inert atmosphere. After cooling to room temperature, the crude product was collected by filtration and washed with ethanol, HCl (3 M) and methanol. Further purification of PAF-40 was carried out by Soxhlet extraction with methanol and THF for 24 h, respectively. The product was dried in vacuum at 120 °C to give PAF-40 in black powder.

Synthesis of PAF-40-Mn and PAF-40-Fe are in a similar procedure.

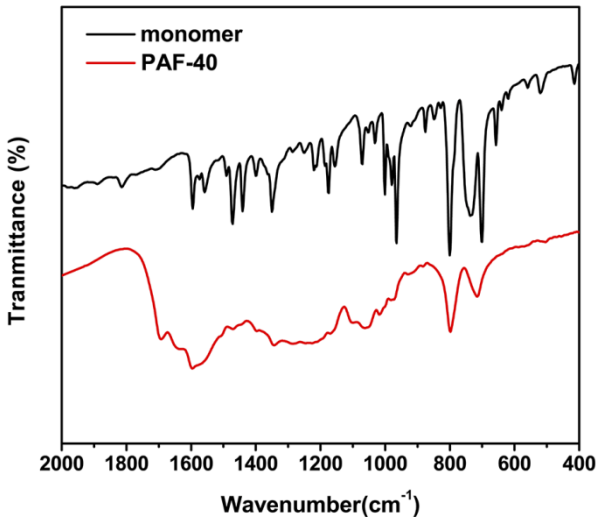

Figure S1. FTIR spectra of monomer (black) and PAF-40 (red).

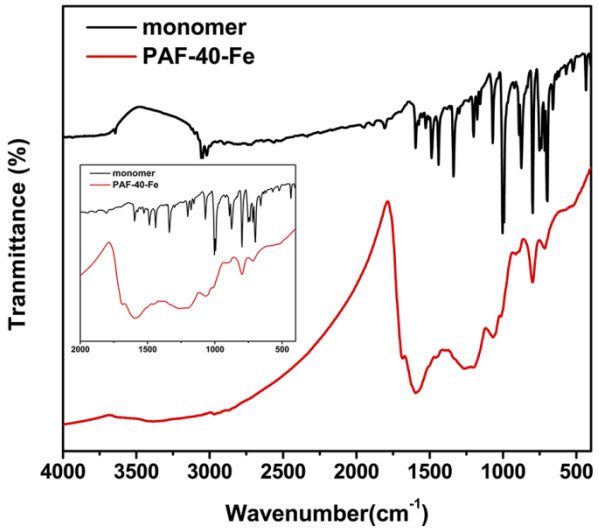

Figure S2. FTIR spectra of monomer (black) and PAF-40-Fe (red).

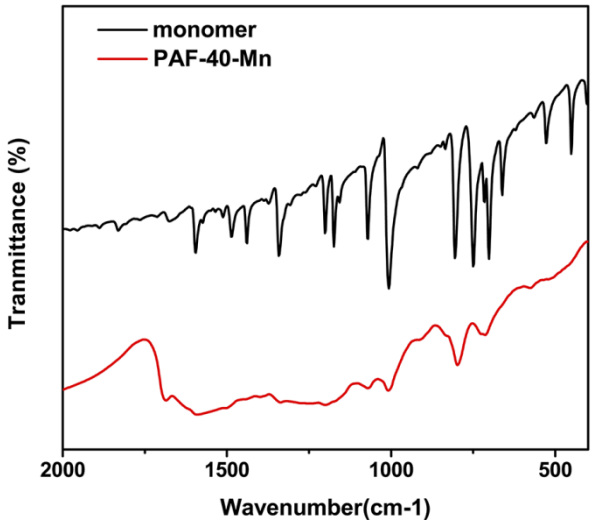

Figure S3. FTIR spectra of monomer (black), PAF-40-Mn (red).

Table S2. Elemental analysis of the PAF-40, PAF-40-Fe, PAF-40-Mn. Fe, Mn and Al contents were determined by ICP.

The measurements of the ICP and elemental analysis on PAF-40s were carried out in order to confirm the composition of the residue in the polymer. Prior to the tests, all products were washed with HCl (1M) and ethanol thoroughly. After that, the samples were dried in the vacuum at 150 ^{o}C for 12 h. At this time, approximately 94% of the elements contained in the PAF networks are determined by three parallel measurements, and the remaining amounts undetected are likely to be chlorine element.

Materials	C (wt %)	H (wt %)	N (wt %)	Fe (wt %)	Mn (wt %)	Al (wt %)
PAF-40	80.16	4.186	7.95			1.475
PAF-40	80.76	4.061	8.04			1.475
PAF-40	79.36	4.043	7.83			1.475
PAF-40-Fe	78.65	4.126	7.95	2.08		1.34
PAF-40-Fe	78.83	4.043	7.87	2.08		1.34
PAF-40-Fe	77.28	4.017	7.83	2.08		1.34
PAF-40-Mn	78.37	4.179	7.44		1.86	1.28
PAF-40-Mn	79.43	4.123	7.53		1.86	1.28
PAF-40-Mn	78.29	4.075	7.42		1.86	1.28

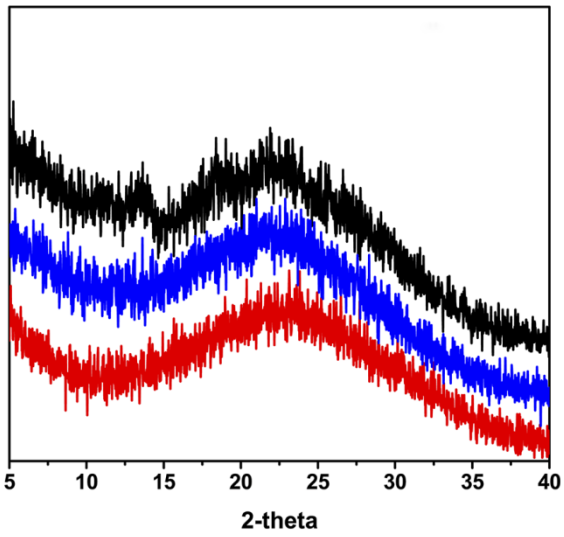

Figure S4. PXRD patterns of synthesized PAF-40 (black), PAF-40-Fe (red), and PAF-40-Mn (blue).

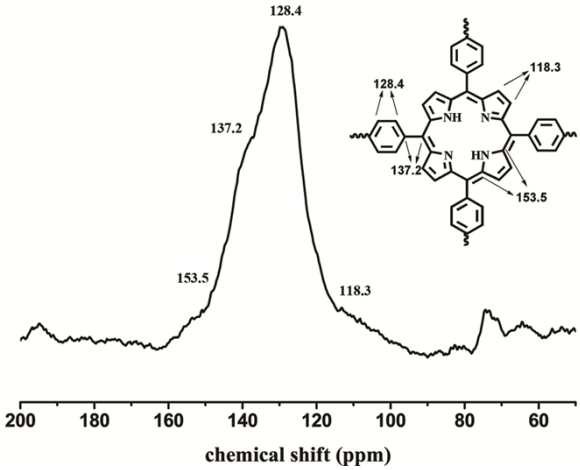

Figure S5. Solid-state ^{13}C NMR of PAF-40.

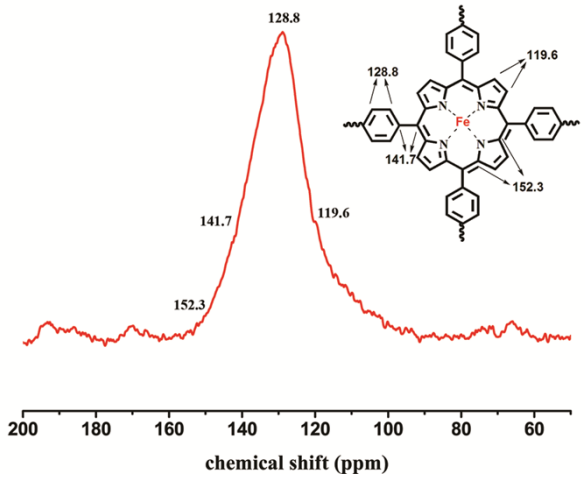

Figure S6. Solid-state ^{13}C NMR of PAF-40-Fe.

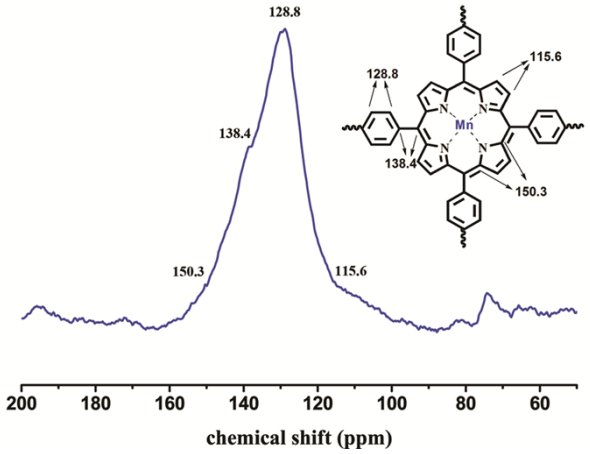

Figure S7. Solid-state ^{13}C NMR of PAF-40-Mn.

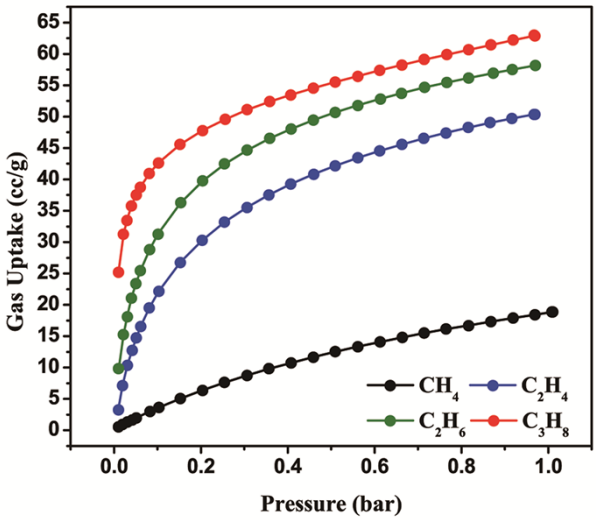

Figure S8. CH_4, C_2H_4, C_2H_6 and C_3H_8 adsorption isotherms of PAF-40 at 273 K.

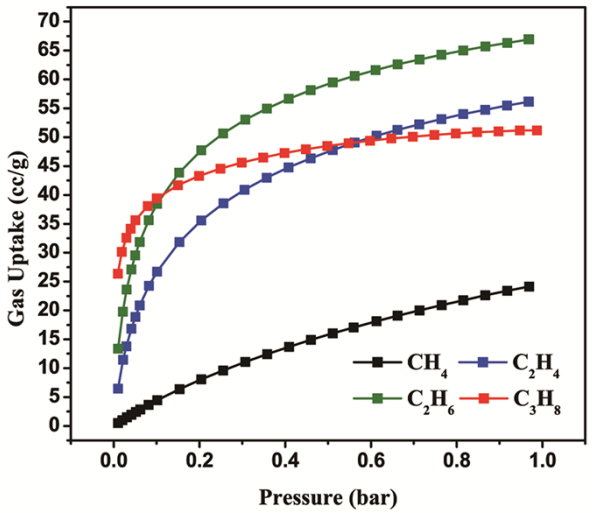

Figure S9. CH_4, C_2H_4, C_2H_6 and C_3H_8 adsorption isotherms of PAF-40-Fe at 273 K.

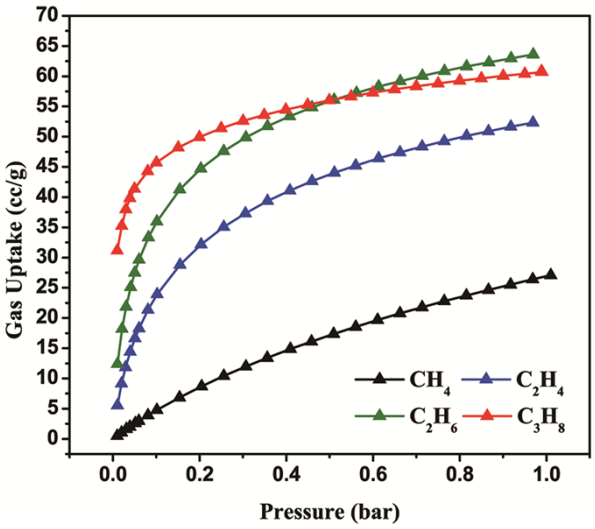

Figure S10. CH_4, C_2H_4, C_2H_6 and C_3H_8 adsorption isotherms of PAF-40-Mn at 273 k.

Calculation of isosteric heat of adsorption

The CH_4 isosteric heat of adsorption of PAF-40 was calculated as a function of the adsorption isotherms at 273K and 298K. The date were modelled with a virial-type expression composed of parameters a_i and b_i (eq 1), and the heat of adsorption was calculated from the fitting parameters using eq 2, where P is the pressure, N is the amount adsorbed, T is the temperature, R is the universal gas constant, and m and n determine the number of terms required to adequately describe the isotherm. a i and b i are virial coefficients.

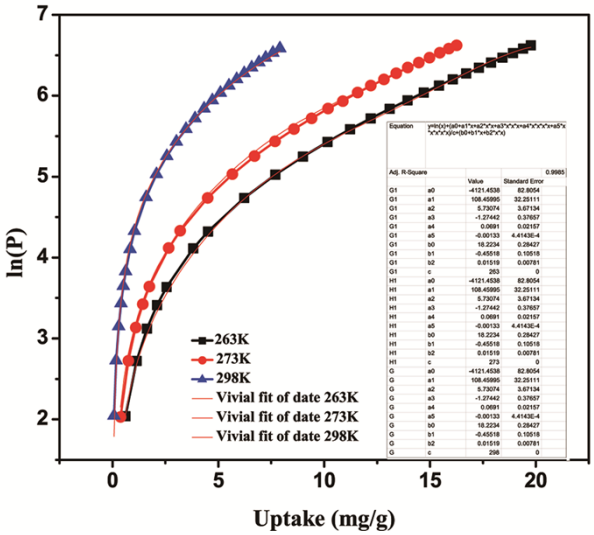

Figure S11. Figure S11. The plots of pressures in function of gas uptakes and the parameters (Virial-type expression) for the calculation of heats of adsorption of CH_4 for PAF-40-Mn..

Calculation of isotherms heat for other small hydrocarbons for PAF-40, PAF-40-Mn and PAF-40-Fe is a similar procedure.

Calculation of CH_4-C_2H_4, CH_4-C_2H_6 and CH_4-C_3H_8 Selectivity for PAF-40 by IAST theory.

The adsorption isotherms for pure CH_4 and C_2H_4, measured at 273 K were first converted to absolute loadings according to Peng-Robinson Equation. In order to perform the IAST calculation, the single-component gas absorption isotherms was fitted by the dual-site Langmuir-Freundlich (DSLF) adsorption model, which was adopted to correlate the pure-component equilibrium data and further to evaluate the adsorption of small hydrocarbons.

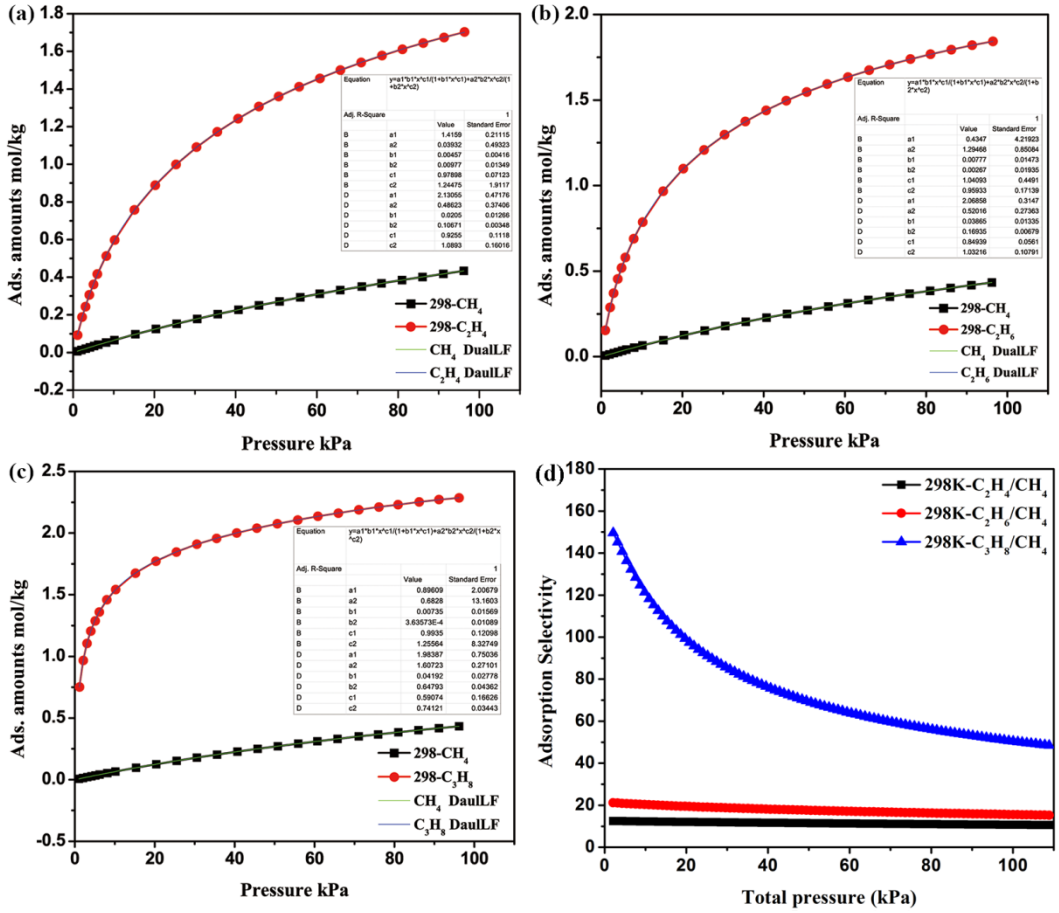

Figure S12. The isotherms are fitted with Langmuir–Freundlich adsorption model-based IAST theory. (a, b and c).The C_2H_4/CH_4, C_2H_6/CH_4 and C_3H_8/CH_4 selectivity for PAF-40 at 298K and 110 kPa by IAST theory (d).

Calculation of gas selectivity for PAF-40-Mn and PAF-40-Fe is a similar procedure.

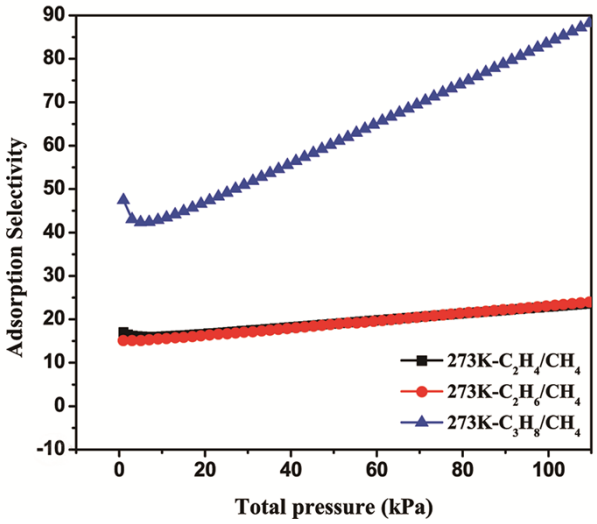

Fig S13. IAST-predicted adsorption selectivity of PAF-40 at 273K and 110kPa.

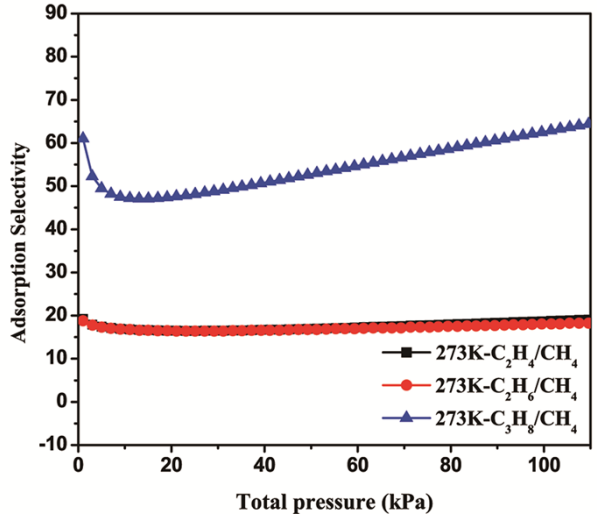

Fig S14. IAST-predicted adsorption selectivity of PAF-40-Fe at 273K and 110kPa.

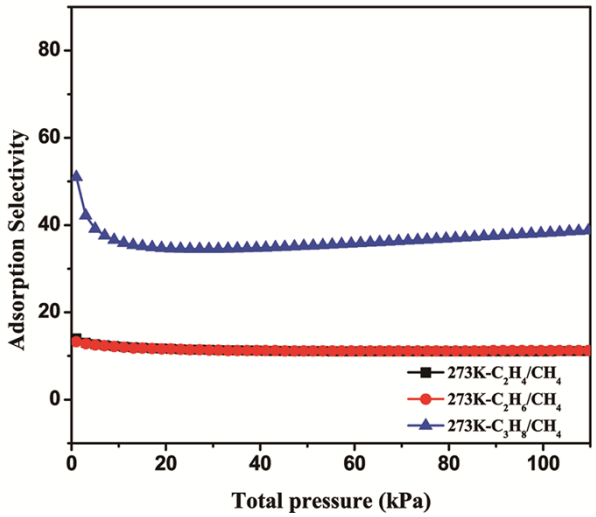

Fig S15. IAST-predicted adsorption selectivity of PAF-40-Mn at 273K and 110kPa.

Table S3 Summary of small hydrocarbons adsorption in porous materials

Materials	T [K]	P [bar]	CH_4 uptake [cm^3/g]	C_2H_4 uptake [cm^3/g]	C_2H_6 uptake [cm^3/g]	C_3H_8 uptake [cm^3/g]	Qst CH_4 [$kJmol^-$]	Qst C_2H_4 [$kJmol^-$]	QstC_2H_6 [$kJmol^-$]
PAF-40	298	1	12	40.4	43.6	53.6	18.2	24.7	36
PAF-40	273	1	18.8	50.3	58.0	63.0			
PAF-40-Fe	298	1	13.8	51.8	41.4	57.9	23.1	30	47.8
PAF-40-Fe	273	1	24.1	56.1	66.9	51.2			
PAF-40-Mn	298	1	11.0	48.8	45.9	56.3	15.5	25.1	34.8
PAF-40-Mn	273	1	27.0	52.3	63.5	60.8			
PCN-14							30		
UTSA-35a	296	1	6.9	60.6	73	130.8	24.4	32.7	36.1
UTSA-36a									
UTSA-5a	296	1	5.2				9.7		
UTSA-5a	273	1	6.9				9.7		
ZJU-48a	296	1	7.8	39.4	43.7				
ZJU-48a	273	1	11.9	65.6	80.6				
COF-1							17		
COF-5							8.5		
HCP-3							20.8		

Reference

S1. S. Ma, D. Sun, J. M. Simmons, C. D. Collier, D. Yuan and H. Zhou, *J. Am. Chem. Soc,* 2008, **130**, 1012-1016.

S2. H. Xu, J. Cai, S. Xiang, Z. Zhang, C. Wu, X. Rao, Y. Cui, Y. Yang, R. Krishna, B. Chen and G. Qian, *Journal of Materials Chemistry A*, 2013, **1**, 9916-9921.

S3. Y. He, R. Krishna and B. Chen, *Energy & Environmental Science*, 2012, **5**, 9107-9120.

S4. Y. He, Z. Zhang, S. Xiang, F. R. Fronczek, R. Krishna and B. Chen, *Chemistry-a European Journal*, 2012, **18**, 613-619.

S5. Y. He, W. Zhou, R. Krishna and B. Chen, *Chemical Communications*, 2012, **48**, 11813-11831.

S6. M. C. Das, H. Xu, S. Xiang, Z. Zhang, H. D. Arman, G. Qian and B. Chen, *Chemistry-a European Journal*, 2011, **17**, 7817-7822.

S7. Y. He, Z. Zhang, S. Xiang, F. R. Fronczek, R. Krishna and B. Chen, *Chemical Communications*, 2012, **48**, 6493-6495.

S8. T. A. Makal, J. Li, W. Lu and H. Zhou, *chem Soc Rev*, 2012, **41**, 7761-7779.